

Kinematics and excitation mechanisms of molecular hydrogen and [FeII] lines in active galactic nuclei

M. G. Pastoriza¹, Alberto Rodriguez-Ardila²,
Sueli Viegas³, T. A. A. Sigut⁴ and Anil K. Pradhan⁵

¹ Departamento de Astronomia, Instituto de Fisica, UFRGS, Av. Bento Gonçalves 9500, C.P. 15051, 91501-970, Porto Alegre, RS, Brazil

² Laboratorio Nacional de Astrofisica/CNPq, Brasopolis, MG, Brazil

³ Instituto de Astronomia, Geofisica e Ciencias Atmosfericas, USP, Sao Paulo, SP, Brazil

⁴ Department of Physics and Astronomy, The University of Western Ontario, London, ON, N6A 3K7, Canada

⁵ Department of Astronomy, The Ohio State University, Columbus, OH, US 43210-1106, USA

Abstract. Near-infrared spectroscopic observations in the range 0.8–2.4 μm are used to study the kinematics and excitation mechanisms of Molecular Hydrogen and [FeII] lines in a sample of AGNs. The width of H_2 lines is narrower than [FeII] lines, therefore they do not originate from the same parcel of gas. The molecular emission is found to be purely thermal but with heating processes which vary among the objects. A clear correlation between $H_2/Br\gamma$ and [FeII] 1.257 $\mu\text{m}/Pa\beta$ is found for our sample objects supplemented with data from the literature. The correlation of these line ratios is a useful diagnostic tool in the NIR to separate emitting line objects by their level of nuclear activity.

1. Introduction

One of the fundamental problems in active galactic nuclei (AGN) research is to determine the dominant excitation mechanisms of the narrow line emitting gas, i.e. whether it is due to non-stellar processes (e.g. photoionization from a central source or shocks from a radio jet) or to stellar processes (e.g. photoionization from OB stars or shocks from supernova remnants). This ambiguity is most evident when interpreting the spectral lines of low-ionization species such as [Fe II] and molecular hydrogen. Both sets of lines are detected in galaxies displaying varying degrees of nuclear activity, from objects classified as starburst-dominated (SD) to those classified as AGN-dominated. Are these lines produced by a unique mechanism in the objects where they are observed, evidencing the so-called AGN-starburst connection? or are they formed by different mechanisms (or some combination thereof) in different classes of objects?

2. Observations

Near-infrared (NIR) spectra from 0.8–2.4 μm were obtained at the NASA 3 m Infrared Telescope Facility (IRTF) with the SpEX spectrometer (Rayner et al. 2003). A $0.8'' \times 15''$ slit was used during the observations, giving a spectral resolution of 360 km s^{-1} . For the objects in which the host galaxy is clearly detected on the DSS images, the slit was oriented along the major axis of the target. Table 1 lists the galaxies in order of right ascension.

Table 1. Observations log and basic properties of the sample. The objects are listed in order of right ascension.

ID (1)	Galaxy (2)	Type (3)	z (4)	$E(B-V)_G$ (5)	Date of Observation (6)	On-source Integration time (s) (7)	Airmass (8)	PA (deg) (9)	r^a (pc) (10)
1	Mrk 1210	Sy2	0.01406	0.030	2002 Apr 25	2700	1.25	58	220
2	Mrk 124	NLS1	0.05710	0.015	2002 Apr 23	2640	1.16	10	990
3	Mrk 1239	NLS1	0.01927	0.065	2002 Apr 21	1920	1.08	0.0	335
4	NGC 3227	Sy1	0.00386	0.023	2002 Apr 23	1920	1.15	0.0	
					2002 Apr 21	720	1.00	158	67
					2002 Apr 25	1080	1.02	158	
5	H1143-192	Sy1	0.03330	0.039	2002 Apr 21	1920	1.31	45	520
6	NGC 3310	SB	0.00357	0.022	2002 Apr 21	840	1.21	158	56
7	NGC 4051	NLS1	0.00234	0.013	2002 Apr 20	1560	1.17	132	37
8	NGC 4151	Sy1	0.00345	0.028	2002 Apr 23	1800	1.10	130	58
9	Mrk 766	NLS1	0.01330	0.020	2002 Apr 21	1680	1.06	112	230
					2002 Apr 25	1080	1.02	112	
10	NGC 4748	NLS1	0.01417	0.052	2002 Apr 21	1680	1.29	36	254
					2002 Apr 25	1440	1.21	36	
11	Mrk 279	NLS1	0.03068	0.016	2002 Apr 24	3600	1.54	0.0	480
12	NGC 5548	Sy1	0.01717	0.020	2002 Apr 23	1920	1.05	112	298
13	Mrk 478	NLS1	0.07760	0.014	2002 Apr 20	3240	1.06	0.0	1200
14	NGC 5728	Sy2	0.01003	0.101	2002 Apr 21	960	1.31	36	160
15	PG 1448+273	QSO	0.06522	0.029	2002 Apr 24	2160	1.01	108	1020
16	Mrk 291	NLS1	0.03519	0.038	2002 Apr 21	2520	1.04	84	550
17	Mrk 493	NLS1	0.03183	0.025	2002 Apr 20	1800	1.07	0.0	500
					2002 Apr 25	900	1.04	0.0	
18	PG 1612+261	QSO	0.13096	0.054	2002 Apr 23	2520	1.10	107	2050
19	Mrk 504	NLS1	0.03629	0.050	2002 Apr 21	2100	1.04	138	570
20	1H 1934-063	NLS1	0.01059	0.293	2002 Apr 21	1200	1.13	150	170
					2002 Apr 25	720	1.17	150	
21	Mrk 896	NLS1	0.02678	0.045	2002 Apr 23	1440	1.21	150	420
					2002 Apr 24	1200	1.18	150	
					2002 Apr 25	1200	1.17	150	
22	Ark 564	NLS1	0.02468	0.060	2000 Oct 10	1500	1.05	0.0	390

^a Radius of the integrated region.

3. Kinematics of the H_2 and [FeII]

The large spectral coverage and medium spectral resolution of our data (360 km s^{-1}) allow us to discuss how the widths of the H_2 lines compares to that of other narrow lines. In Figure 1 we presents a comparison of the lines profile of [FeII] $1.257 \mu m$ (full histogram) and H_2 $2.122 \mu m$ for Mrk 1210, for which the observed profile of $Br\gamma$ (solid line) has also been plotted. The smaller values of the FWHM of H_2 relative to other narrow lines suggest that the molecular gas is concentrated in the external/extended NLR or possibly even in the host galaxy, where the gravitational effects of the black hole on the emitting gas are lower than in the BLR. This scenario seems unlikely, however, because for the large majority of the objects the size of the integrated region covered by the spectra is no larger than 500 pc. The alternative is to consider that the molecular gas is not kinematically linked to the NLR gas even though the two are co-spatial.

4. Excitation mechanisms of the NIR H_2 lines

The Fig. 2 shows: (a) 2-1S(1)/1-0S(1) vs 1-0S(2)/1-0S(0) and (b) 2-1S(1)/1-0S(1) vs 1-0S(3)/1-0S(1). These diagnostic diagrams have been proposed by Mouri (1994). Curves represent thermal emission at 500-3000 K. Crosses are the non-thermal UV excitation models of Black & Van Dishoek (1987). Open circles are thermal UV excitation models of Sternberg & Dalgarno (1989). The numbers identify each object according to the notation given in column 1 of Table 1. The black square in (a) represents the datum for NGC 253, a typical starburst galaxy, taken from Harrison *et al.* (1998). A large scatter is observed in both line ratios for the galaxy sample. NGC 3227, NGC 4051, NGC 4151 and Mrk 766 (labelled 4, 7, 8 and 9, respectively) fall near the thermal curve model and indicate excitation temperatures for the thermal component of between 1500 and 2500 K. For these galaxies, the H_2 emission can be considered purely thermal. For the remaining

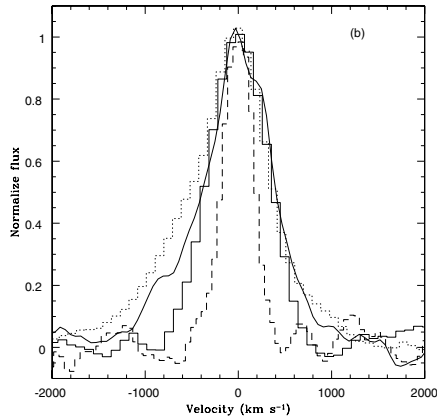


Figure 1. Comparison of the line profiles of [FeII] 1.257 μm (full histogram) and H_2 2.122 μm for Mrk 1210, for which the observed profile of $Br\gamma$ (solid line) has also been plotted.

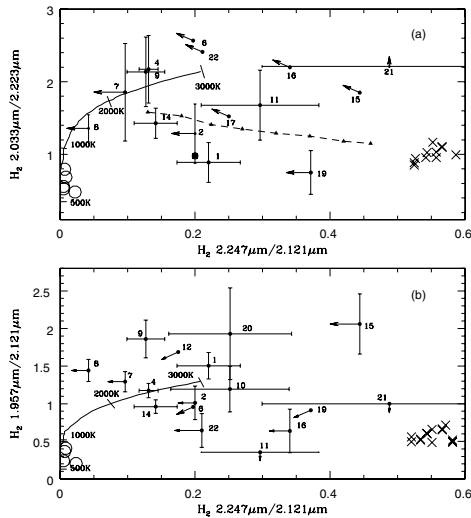


Figure 2. Plot of (a) 2-1S(1)/1-0S(1) vs 1-0S(2)/1-0S(0) and (b) 2-1S(1)/1-0S(1) vs 1-0S(3)/1-0S(1). Curves represent thermal emission at 500-3000 K. Crosses are the non-thermal UV excitation models of Black & Van Dishoeck (1987). Open circles are thermal UV excitation models of Sternberg & Dalgarno (1989). The numbers identify each object according to the notation given in column 1 of Table 1. The black square in (a) represents the datum for NGC 253, a typical starburst galaxy, taken from Harrison et al. (1998)

objects, a mixture of thermal and non-thermal processes are probably at work, with the excitation temperature of the thermal component higher than 1000 K. Interestingly, no AGN is located in the region occupied by the pure non-thermal UV excitation models, except possibly Mrk 896

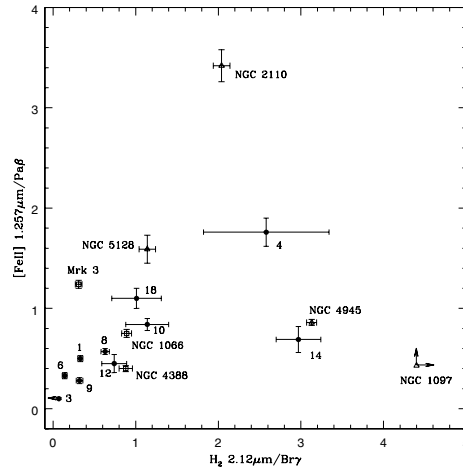


Figure 3. The ratios H_2 2.121 $\mu\text{m}/\text{Br}\gamma$ and $[\text{FeII}]$ 1.257 $\mu\text{m}/\text{Pa}\beta$. Only the Seyfert 1s and NLS1 in which a reliable deblending of the narrow component of the HI lines was carried out are plotted. Filled circles represents our data and open symbols data taken from the literature. Triangles are measurements from Knop *et al.* (1996) and squares from Reunanen *et al.* (2002). The number along each data point identifies our galaxies according to the notation given in column 1 of Table 1.

5. Are the $[\text{FeII}]$ and H_2 related

The observational evidence indicates that $[\text{FeII}]$ and H_2 are common features in the nuclear spectra of AGN, although probably originated from different parcels of gas. However, this does not exclude the possibility that both sets of lines originate from a single, dominant mechanism. Moreover, if dust is intermixed with the line emitting clouds, and there are strong velocity gradients, $[\text{FeII}]$ and H_2 lines can appear to have different velocity fields even though they are produced in adjacent regions.

If $[\text{FeII}]$ and H_2 have a common origin, a strong correlation between their observed fluxes should be expected. The Figure shows the correlation between H_2 2.121 $\mu\text{m}/\text{Br}\gamma$ and $[\text{FeII}]$ 1.257 $\mu\text{m}/\text{Pa}\beta$ for our sample. Only the Seyfert 1s and NLS1 in which a reliable deblending of the narrow component of the HI lines was carried out are plotted in Fig. 3. Filled circles represent our data and open symbols data taken from the literature. Triangles are measurements from Knop *et al.* (1996). and squares from Reunanen *et al.* (2002). The number along each data point identifies our galaxies according to the notation given in column 1 of Table 1.

References

- Black, J. H., & van Dishoeck, E. F. 1987, *ApJ*, 322, 412
 Harrison, A., Puxley, P., Russel, A., & Brand, P. 1998, *MNRAS*, 297, 624
 Knop, R. A., Armus, L., Larkin, J. E., Matthews, K., Shupe, D. L., & Soifer, B. T. 1996, *AJ*, 112, 81
 Mouri, H. 1994, *ApJ*, 427, 777
 Rayner, J. T., *et al.* 2003, *PASP*, 155, 362
 Reunanen, J., Kotilainen, J. K., & Prieto, M. A. 2002, *MNRAS*, 331, 154
 Sternberg, A., & Dalgarno, A. 1989, *ApJ*, 338, 197